

Active Site Structure of Cu/ZSM-5: Computational Study

Kazuo Teraishi,^{*,†} Masaya Ishida,[‡] Jun Irisawa,[§] Masayoshi Kume,[⊥] Yoshiyuki Takahashi,^{||} Takashi Nakano,[#] Hiroyuki Nakamura,[@] and Akira Miyamoto^{||}

Tonen Co. Research & Development Laboratory, 1-3-1 Nishitsurugaoka, Oimachi, Iruma-gun, Saitama-ken, 356, Japan

Received: March 17, 1997; In Final Form: June 2, 1997[⊗]

The coordination structures of Cu ionic species in ZSM-5 zeolite were investigated by molecular dynamics (MD) simulations and molecular orbital (MO) calculations. Al sites were first sought so as to reproduce the square-planar coordination of Cu(II), which is well characterized by the ESR spectra. When two Al's occupy T8 sites in the six-membered ring, the calculated coordination of Cu(II) agreed well with the experimental data. For this Al siting, Cu(II)–O–Cu(II) and two Cu(I)'s were respectively simulated, and the coordination of the former species was found to be consistent with the EXAFS results. Furthermore, from the MO calculation Cu–O–Cu was anticipated to be very reactive and thus might be the active site. The function of zeolite would therefore be the stabilization of this species. On the other hand, Cu dimer was found unstable, and the reaction mechanism based on it was supposed unlikely.

Introduction

Since Iwamoto discovered the unique activity of Cu/ZSM-5 in NO direct decomposition to $\text{N}_2 + \text{O}_2$,¹ many academic as well as industrial researchers have been engaged in the study of this catalyst from both environmental concerns and scientific interests. Despite these efforts, its complicated catalytic behavior left the reaction mechanism still controversial. A consensus has been attained upon the points that Cu ionic species are the active sites and their redox chemistry plays a crucial role in the reaction. However, uncertainty still remains in their coordination structure and oxidation states, and whether they are monomer or dimer under the working conditions. Among the types of zeolites examined,² e.g., Y, MOR, and FER, why only MFI exhibits a high activity is also still unclear and the role of the framework should be elucidated. The grasp of the Cu ionic species in this catalyst should therefore be a first step toward understanding the reaction mechanism, and numerous experimental measurements such as ESR, EXAFS, photoluminescence, and IR have been performed^{3–11} for this purpose.

The coordination of Cu(II) ions in the calcined samples were confirmed by many authors^{3–6} to be square planar and square pyramidal using ESR spectroscopy. Grünert et al.⁴ used EXAFS to investigate the environment of Cu in the calcined samples and found that the spectra were dominated by a Cu–O distance of 1.93–1.96 Å with a coordination number (CN) of 5–6. Also a feature corresponding to a Cu–Cu bond at 2.95 Å with a CN of 1 was observed, which was assigned to $[\text{Cu}(\text{O}=\text{Cu})]^{2+}$ oxocation. The existence of $[\text{Cu}(\text{O}=\text{Cu})]^{2+}$ was also confirmed by H_2 TPR.⁷ The maximum activity in NO decomposition is attained, however, when the catalysts are pretreated in nitrogen or in vacuum, which results in the reduction of Cu(II) to Cu(I). The presence of Cu(I) was confirmed by photoluminescence,^{6,8} IR spectra of adsorbed CO and NO,^{7,9–11} and Auger kinetic

energy measurements.⁴ The EXAFS spectra of the activated samples⁴ were characterized with the decreased CN of Cu–O to 2.5–3.5, while the distance as well as the contribution from the Cu–Cu bond remain unchanged.

Computational simulations have also been applied to study the active site of this catalyst. Molecular dynamics (MD) has been applied to study zeolites in many cases for its capability to treat the crystal as a whole. Sayle et al.¹² simulated the adsorption of Cu(II) and Cu(I) on the silicalite by MD and found that the most favorable positions are near T12 and T7, respectively. The nearest-neighbor Cu–O distance of 2.02–2.14 Å with a CN of 4 corresponds well with the experimental observations. However, the strong binding energy of Cu–Al, which was discovered from another simulation of Cu(II) adsorbed on ZSM-5 with the T12 site substituted by Al, suggests that Cu's are mostly associated with Al sites. But the structure obtained from the latter simulation was fairly distorted and did not correspond with the experimental data. Molecular orbital (MO) analysis has also been used particularly when the chemical reactions are involved, since it solves the electronic state explicitly while MD calculates only the motion of nuclei using the empirical force parameters that express the interaction between them. The drawback of MO is a demand for high computational resources, which often limits the system to be a small cluster. The interaction between NO and Cu is more chemical than physical, in other words, electron transfer is involved. Yokomichi et al.¹³ calculated the adsorption of NO on Cu by means of DFT and reproduced the IR frequency from the vibrational analyses. Recently Bernhardt et al.¹⁴ investigated thoroughly the reaction path of NO decomposition occurring over the single Cu^+ adsorbed at the single (T12) Al site. Although they proposed some plausible reaction pathways, they did not give any explanations as to why only ZSM-5 reveals a high activity, which is a key point from the viewpoint of designing a noble catalyst.

As mentioned above, Cu cations are the active sites and they are associated with the negatively charged Al sites in the molecular sieve. Experimental determination of Al sites is, however, difficult because Al and Si cannot be distinguished by X-ray for their similar electron densities. In the present study, Al sites which reproduce the Cu(II) coordination observed by experiments, namely, square planar, was searched for at first

[†] Tonen Co. Research & Development Laboratory.

[‡] Sumitomo Chemical, 6, Kitahara, Tsukuba, Ibaraki, 300-32, Japan.

[§] Asahi Glass, 1150, Hazawacho, Kanagawaku, Yokohama, 221, Japan.

[⊥] Toa Gosei, H, Funamicho, Minatoku, Nagoya, 455, Japan.

^{||} Nippon Shokubai.

[#] Mitsui Toatsu, 1190, Kasamacho, Sakaeku, Yokohama, 247, Japan.

[@] Japan Energy, 3-17-35, Niizo-Minami, Toda, Saitama, 335, Japan.

^{||} Tohoku University, Aoba, Aramaki, Aoba-ku, Sendai, 980-77, Japan.

[⊗] Abstract published in *Advance ACS Abstracts*, August 15, 1997.

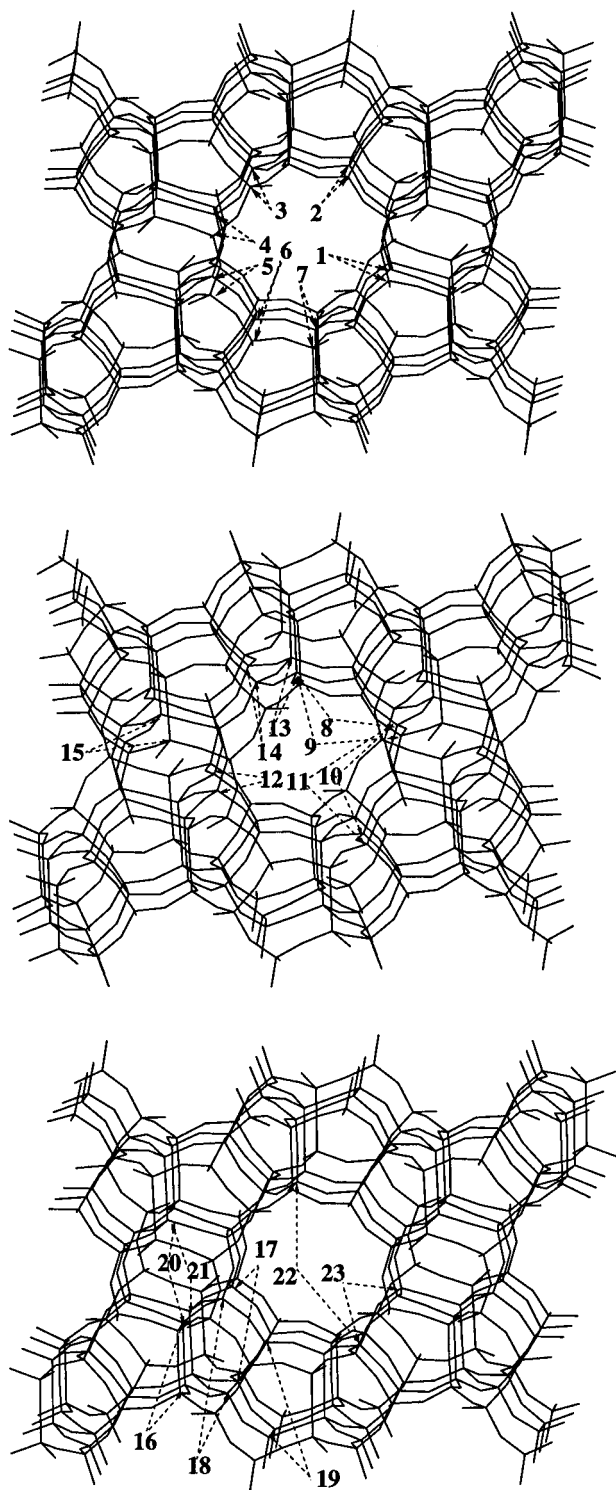


Figure 1. Al substitution sites of 23 Al configurations.

by means of MD simulations. We found that when two Al's occupy T8 sites in the six-membered-ring, the calculated coordination structure of Cu(II) agrees well with the experimental data. Accordingly, for this Al siting Cu(II)—O—Cu(II) and two Cu(I)'s were respectively simulated. The coordination of the former species was found to be consistent with the EXAFS data, particularly on the Cu—Cu distance. Furthermore, *ab initio* MO calculations were performed on the cluster models extracted from the structures obtained by MD. The electronic structure of Cu—O—Cu suggested a high reactivity. We inferred that this oxocation is the active site, and zeolite functions as the support of this reactive species. To examine the possibility the Cu(I) dimer, photoluminescence spectra corresponding to

TABLE 1: Al Substitution Sites of 23 Al Configurations

model	Al sites		model	Al sites		model	Al sites		model	Al sites	
1	T11	T11	7	T3	T3	13	T3	T9	19	T2	T5
2	T8	T8	8	T7	T9	14	T6	T12	20	T4	T10
3	T6	T6	9	T7	T9	15	T4	T4	21	T4	T4
4	T5	T5	10	T7	T12	16	T9	T10	22	T9	T12
5	T1	T1	11	T7	T12	17	T7	T12	23	T5	T12
6	T2	T2	12	T1	T7	18	T1	T6			

the relaxation from the excited triplet state (phosphorescence) was calculated and compared with the experimental data. Also Cu(I) dimer bridged by NO was studied. None of these calculations, however, suggested the existence of Cu(I) dimer.

Calculation

To determine the Al sites that reproduce the square-planar coordination of Cu(II), 23 Al configurations, which satisfy Lowenstein's rule (i.e., no neighboring Al's directly bonded by one oxygen) but have Al's close to each other, were examined (Figure 1 and Table 1). In these models, two unit cells of MFI stacked along the *c* axis were taken as a simulation cell, and in this simulation cell only two T sites were substituted by Al while all others were kept Si. These simulation cells are hypothetically stacked periodically in the three-dimensional space up to infinity, which was accomplished by the Ewald sum method in the calculation. One Cu(II) was then placed somewhere close to the Al site by hand, and the coordination structure was calculated by the procedure described below. For the most reasonable Al configuration found from these simulations (T8 sites), Cu(II)—O—Cu(II) and two Cu(I)'s were simulated respectively to obtain the adsorption structures.

On the basis of the coordination structures determined by MD, *ab initio* MO calculations were performed for Cu(II), Cu(II)—O—Cu(II), and two Cu(I)'s adsorbed on the cluster models having Al substitutions at T8 sites (Figure 2). For the first two species, a six-membered-ring cluster with OH termination was used, while for the last one, since one Cu(I) was predicted to fall out of the six-membered ring by the MD simulation, a larger cluster was chosen. The initial geometry of these clusters were extracted from the structures determined by MD (Figure 3a, 4), where the terminal H's were placed along the O—Si bond with the OH length of 0.946 Å. In the case of two Cu(I)'s, some Si atoms far from Cu ions were terminated directly by H instead of OH (Figure 2c). In this case H atoms were placed along Si—O bond with a bond length of 1.474 Å. Geometry optimizations were performed while terminal OH's (or H's) were nailed at the initial positions.

To examine the existence of Cu(I) dimer, photoluminescence spectra corresponding to the relaxation from the excited triplet state (phosphorescence) was calculated. The optimized structure of two Cu(I)'s in the ground state was reoptimized in the triplet state employing the same cluster mode (Figure 5a). Also for the comparison, single Cu(I) coordinated to the same zeolite model but only one Al site instead of two (Figure 5b) was calculated in the triplet state. At the triplet state geometry, the singlet state wave function was solved, and the excitation spectrum from singlet to triplet was calculated by the single excitation configuration interaction method (CIS), which we regarded here as the photoemission spectrum from triplet to singlet. Furthermore, from the expectation that Cu(I) might dimerize if NO is adsorbed, two Cu(I)'s bridged by NO was examined using the same cluster model as that used for two Cu(I)'s (Figure 6). The initial structures of the Cu(I) dimer bridged by NO through N and through O were constructed based

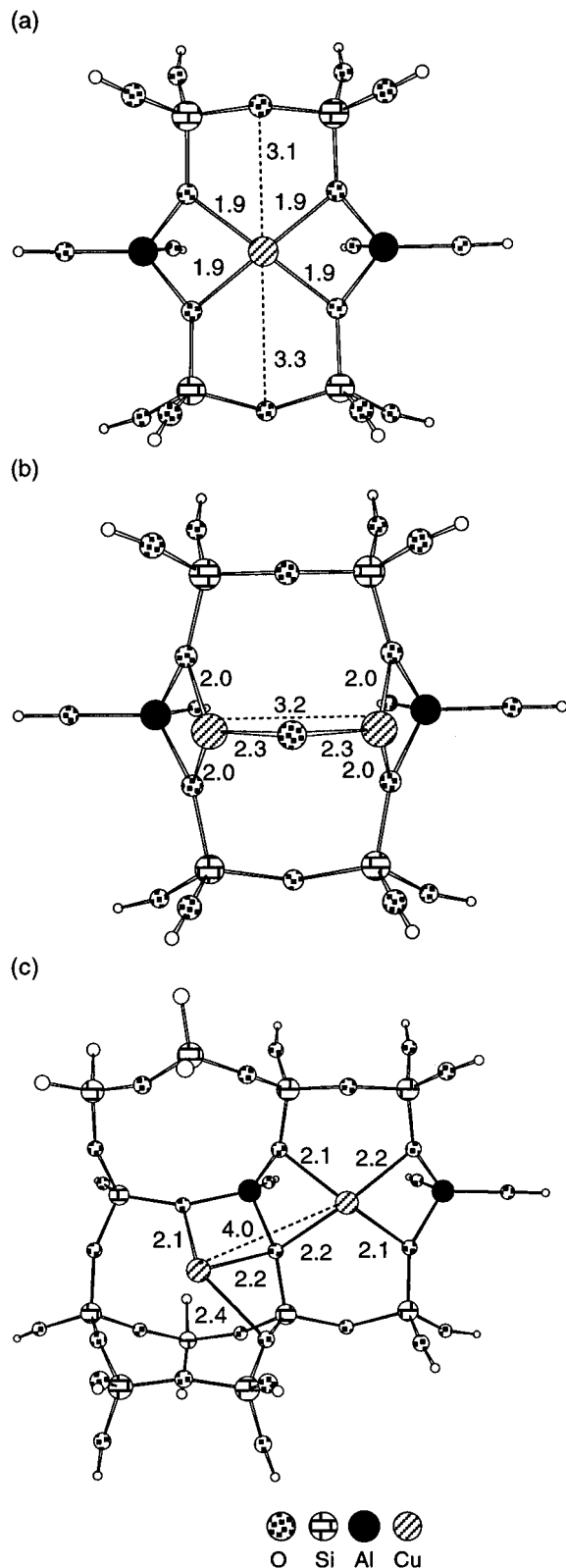


Figure 2. Cluster models used for MO calculations and the optimized structural data (Å). (a) Cu(II) adsorbed on the six-membered ring with two T8 sites substituted by Al. (b) $[\text{Cu}-\text{O}-\text{Cu}]^{2+}$ adsorbed on the same cluster as (a). (c) Two Cu(I)'s adsorbed on the cluster consisting of the same six-membered ring as in (a) as well as the other parts in the interaction with the Cu(I) fallen out of the six-membered ring.

on the structure of $\text{Cu(II)}-\text{O}-\text{Cu(II)}$. Geometry optimizations of both structures lead to the same structure where NO is adsorbed on the single Cu(I) through O (Figure 6a). Adsorption through N on the single Cu(I) was also calculated for comparison (Figure 6b).

MD simulations proceeded from the equilibration stage at 300 K for 10 ps with the time step of 2 fs (5000 steps), followed by cooling at the pace of -1 K/step up to 10 K (290 steps), and final stabilization at 10 K for 710 steps. The force parameters were taken from Sayle,¹² where oxygen atoms were also treated as rigid ions, instead of the shell model which was adopted in the original paper. This adaptation may be approved because the crystal structure of zeolite was still well maintained. No constraints were imposed on the motion of all atoms. The level of MO calculations was compelled to be primitive because of the large cluster size. The minimal basis set with effective core potential (LANL2MB) was employed, and no electron correlation effects were taken into account, i.e., RHF for singlet state and ROHF for doublet and triplet states. MXDORTO¹⁵ and Gaussian 94¹⁶ were used for MD and MO calculations, respectively.

Result

Some typical adsorption structures of Cu(II) are given in Figure 3. Only the vicinities of Cu(II) and Al are shown, although the entire crystal was included in the calculations. The coordination structures of models 1, 2, and 21 are almost identical, and only model 2 is shown here (Figure 3a). Out of the similar models 3, 5, 7, and 15, model 15 is presented (Figure 3b). Model 11 (Figure 3c) was chosen from the similar models 9 and 11. Models 13, 14, 18, and 19 were represented by model 14 (Figure 3d). The structures of models 16 and 23 are respectively shown in Figure 3e,f. The structural data of the other models are not shown here for the apparent dissimilarity with the experimental findings as well as energetic disadvantage, and they will not be touched upon in the following discussion. The structures of models 1, 2, and 21 reproduced the square-planar coordination of Cu(II) and the structure of model 2, which gave the lowest energy among the three, was further investigated. The six-membered ring consisting of two T8 sites as well as four other T sites was taken as a cluster model to be subjected to the MO calculation, and the optimized structure is given in Figure 2a.

$\text{Cu(II)}-\text{O}-\text{Cu(II)}$ and two Cu(I)'s were respectively simulated in the model where two T8 sites of the same six-membered ring were replaced by Al. The adsorption structures obtained by MD are given in Figure 4. Here also only the vicinities of Cu ions are shown. Clusters were then extracted from the respective structures as described in the calculation section, and MO calculations were carried out. The structural data of the optimized geometry are given in Figure 2b,c. The structures of Cu(I) dimer and monomer in excited triplet state are shown in Figure 5a,b, respectively. Geometry optimization of the Cu(I) dimer bridged by NO through N and through O both lead to the same structure where NO is adsorbed on the single Cu(I) through O (Figure 6a). Calculated adsorption structure of NO through N on the single Cu(I) is given in Figure 6b.

Discussion

Cu(II). Square-planar coordination of Cu(II) was obtained when two T8, T11, or T4 sites in the six-membered ring were replaced by Al (Figure 3a). Models 1 and 2 also gave the lowest energies of all considered models with a slight preference of the latter, although the absolute value of the difference in energies of different models does not bear a physical meaning, since the parameters used here were determined to reproduce the structure and not, e.g., the heat of formation. Cu-O distances of this model are also in good agreement with EXAFS data. The T12 site is often considered as the most preferable Al substitution site in ZSM-5. But T12 sites are directly connected

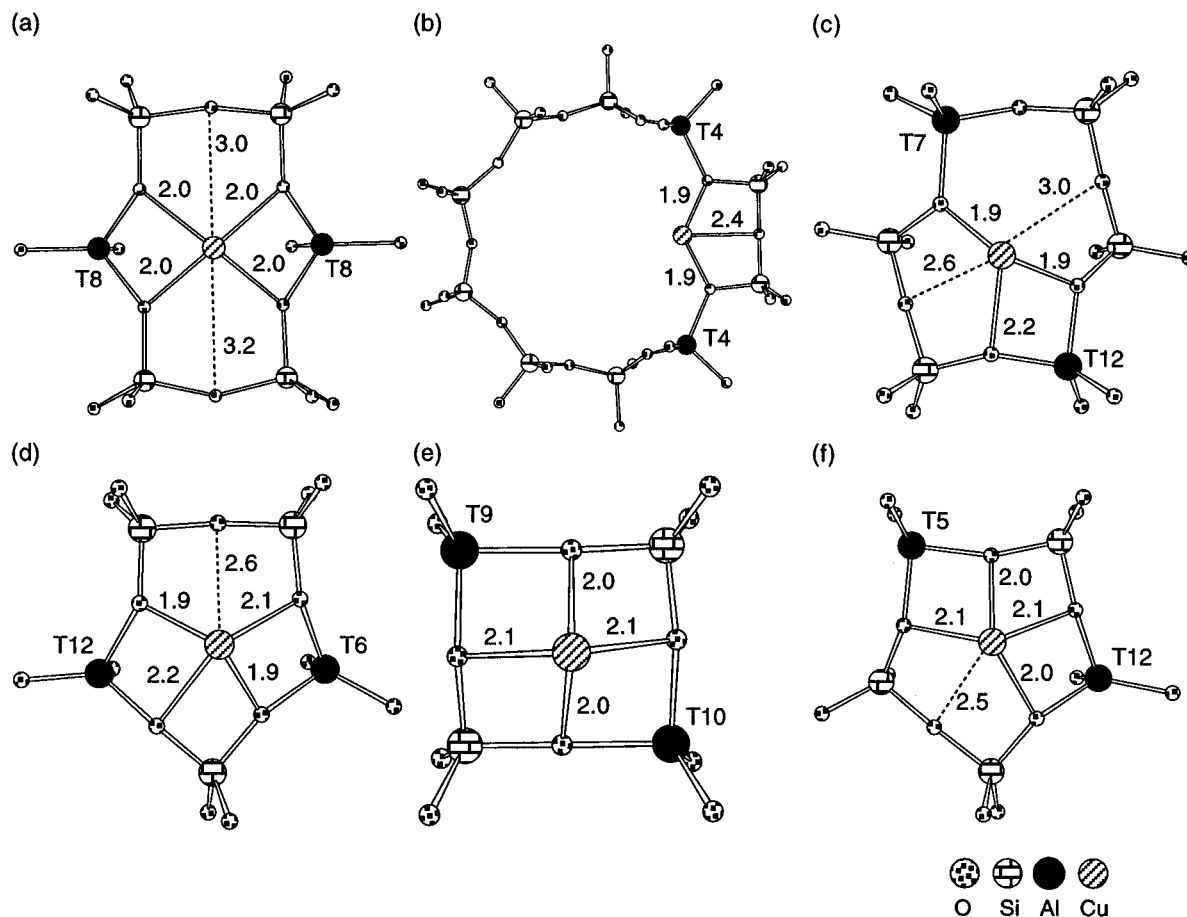


Figure 3. Coordination structures of Cu(II) in model 2 (a), model 15 (b), model 11 (c), model 14 (d), model 16 (e), and model 23 (f) calculated by MD. Only the vicinity of Cu ion and Al sites are shown.

to each other via a single oxygen and the simultaneous substitution of two T12 sites by Al are not allowed due to Lowenstein's rule. When T12 and T7 in the same six-membered ring are substituted (Figure 3c), the coordination structure of Cu(II) is fairly distorted and cannot be regarded as square pyramidal or square planar. When T12 and T6 (Figure 3d) or T12 and T5 (Figure 3f) in the same five-membered ring are substituted, Cu(II) coordinates to four oxygens at distances of 1.9–2.2 Å and to an additional one at 2.5–2.6 Å. This structure may be seen as a slightly distorted square pyramid. The five-membered rings considered here form the second lowest energy group following the six-membered rings. When the diagonal positions of the four-membered ring are substituted by Al (Figure 3e), though the coordination is square pyramidal, Cu is far from the plane defined by four oxygens and the stability is poor. Also investigated was when two positions of 10-membered ring are substituted by Al (Figure 3b). Cu is tri- instead of tetra-coordinated, which contradicts the experimental observations. From the above results and the fact that MFI contains a considerable number of six- and five-membered-rings, we may conclude that square-planar signals are associated with the Cu(II) adsorbed on the six-membered ring where T8, T11, or T4 are substituted by Al, while square-pyramidal signals originate from the Cu(II) adsorbed on the five-membered ring. We also infer that the superior performance of ZSM-5 is due to the high density of five- and six-membered rings. The weakness of the present calculation is, however, the negligence of water and/or hydroxyl ions. Dedeczek⁶ proposed that the square-planar coordination was formed from the $(\text{Cu(II)}-\text{OH}^-)^+$ precursor balanced by a framework Al site. This possibility will be examined in the future study.

There have been a considerable number of studies on Al siting in MFI zeolite, but a consensus has not been reached. Derouare et al.¹⁷ calculated the Si/Al substitution energies by means of the ab initio MO method. The cluster of each T site was taken from the crystal structure, and the models when this site is Si and when it is Al were considered. From the comparison of the energetic differences between them, they concluded that T12 is the most preferable substitution site, which is still believed by many researchers today. Swaisgood et al.¹⁸ carried out similar calculations but with a larger basis set and found that T6 is the most favorable substitution site, followed by T12 and T9 with slightly less stability. The size of the clusters used in these calculations were limited to be small because of the high computational cost of ab initio MO methods. Chatterjee et al.¹⁹ sacrificed the computational accuracy to extend the cluster size and adopted the MNDO semiempirical MO method. Their results with pentameric clusters revealed that T4 and T8 are the most preferred substitution sites. Blanco et al.²⁰ also conducted MNDO calculations, but they used a different approach to calculate the Si/Al substitution energy. They calculated the Si/Al substitution energies of the rings of which a particular site is a member, and added them up with the appropriate weights. They found that T9 is the most favored substitution site, while T4, T11, T6, and T8 are slightly unfavored compared to T9. Schröder et al.,²² on the other hand, performed the classical defect energy calculations and concluded from the small differences found in the calculated replacement energies that Al's distribute over a broad range of framework even at low temperatures. Therefore the previous works using sufficiently large models do not contradict our conclusion that substantial amount of T8 sites (as well as T11 and T4) are

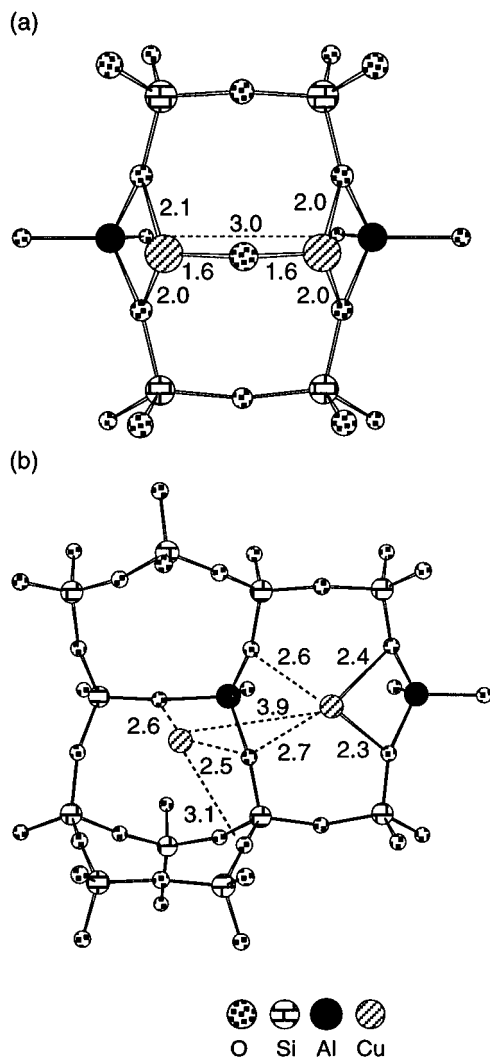


Figure 4. Coordination structures of Cu(II)-O-Cu(II) (a) and two Cu(I)'s (b) in model 2 calculated by MD. Only the vicinity of Cu ions and Al sites are shown.

occupied by Al and Cu(II) prefers to be adsorbed at these sites, which are the species detected by experiments. This Al configuration thus deserves further investigations.

The adsorption structure of Cu(II) was calculated by ab initio MO using a six-membered-ring cluster with two T8 sites substituted by Al (Figure 2a). Though the calculation level is rather primitive, no empirical parameters were used in this calculation on the contrary to MD. Very good agreement was achieved between the structures calculated by MO and MD, which verifies the force field parameters used here for Cu(II) as well as framework atoms, Si, Al, and O.

Cu(II)-O-Cu(II). On the basis of the assumption that Cu ions stay at the proximity of the initial Cu(II) position after the activation treatment, the activated Cu species were investigated near T8 sites. First, Cu(II)-O-Cu(II) was simulated in ZSM-5 with two T8 sites replaced by Al. The calculated Cu-O-Cu structure was in good agreement with the EXAFS data taken after the activation process, i.e., tricoordination of O around Cu and particularly Cu-Cu distance of 3 Å. The Cu-O distance of the Cu-O-Cu group is slightly shorter, but this may be due to the inadequacy of MD parameters as explained below. From the following simulation it was found that two Cu(I) cannot form a dimer at this distance, and we may therefore conclude that the substance which gives rise to a peak associated with Cu-Cu at 3 Å is Cu-O-Cu. Our simulation would serve as another clue for the existence of this oxocation.

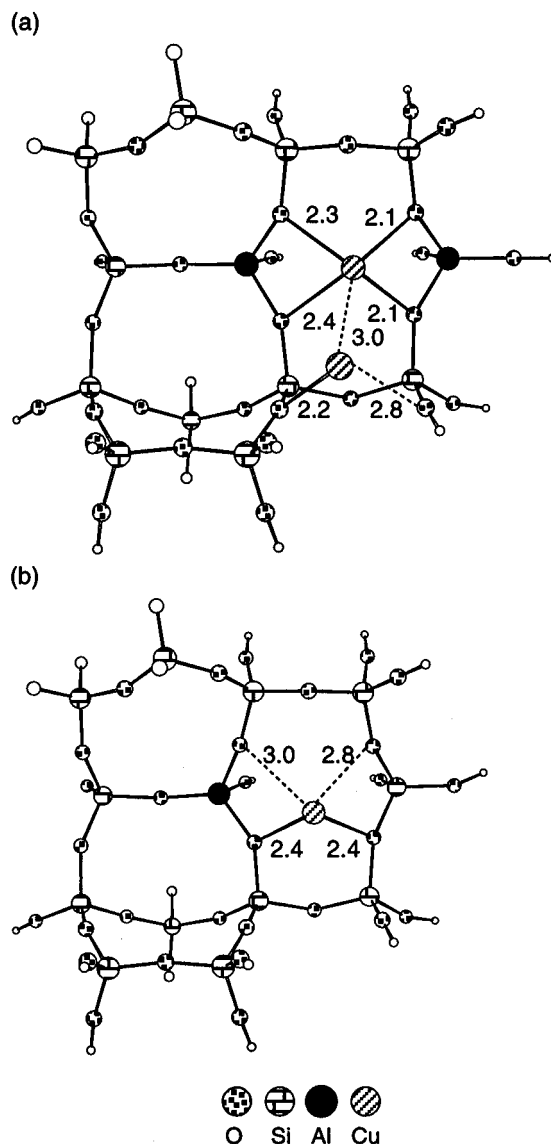


Figure 5. Excited-state structures of Cu(I) dimer (a) and monomer (b) adsorbed on the same cluster model as Figure 2c (with one Al replaced by Si in the case of (b)).

Cu-O-Cu adsorbed on the six-membered ring was calculated by ab initio MO in both singlet and triplet states. The latter was calculated to be 80 kcal/mol more stable than the former, thus it is safe to conclude from this large energy difference that the triplet state is the ground state even taking into account the poor accuracy due to the primitive computational level used here. The structure obtained by MO (Figure 2b) was similar to that obtained by MD (Figure 4a), except for the local structure of the Cu-O-Cu group. The Cu-O bond length of the structure obtained by MO is 0.7 Å longer than that obtained by MD and Cu-O-Cu angle is more acute. The disagreement between the Cu-O-Cu structures obtained by MD and by MO is probably due to the abnormal atomic charges on this group. The Mulliken atomic charges on the framework oxygens fall in the range between -0.5 and -0.7 au with the calculation level used here. The bridging oxygen, on the other hand, was found to bear a positive charge of 0.19 au, which is apparently different from the framework ones and indicates a necessity for a different set of parameters for this particular species.

Further attention should be paid to the electronic structure of the Cu-O-Cu group. The Mulliken atomic charge on Cu is 0.33 au, a much smaller value than 0.81 au of the Cu(II)

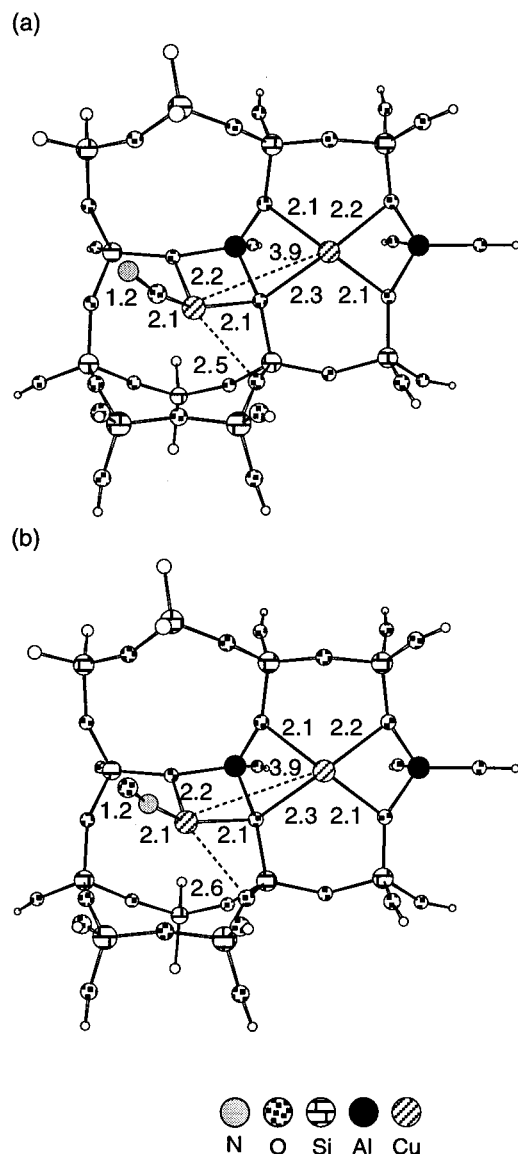


Figure 6. NO adsorption structure on Cu(I) through O (a) and through N (b) calculated by MO. Cluster model is the same as Figure 2c.

coordinated to the six-membered ring and even smaller than 0.43 au and 0.58 au of Cu(I) found in the following calculation. These abnormal charges on Cu and O indicate that the Cu ions of the Cu–O–Cu group draw electrons from the bridging oxygen and leave themselves much less positive than Cu(II) or even Cu(I). If NO is adsorbed onto this Cu, electron will be back-donated to a NO antibonding p orbital which would result in a weakening of the NO bond. At the same time, the oxygen atom becomes less ionic or more like a neutral atom, which is also suggested from the fact that the spin density is localized on this bridging O. This atomic oxygen will then attack the activated NO to complete the following disproportionation step proposed by Beutel.⁷



The role of the zeolite may thus be to disperse these reactive species which otherwise would react with each other.

Cu(I). Two Cu(I)'s were also simulated in ZSM-5 with two T8 sites substituted by Al. Simulation revealed that two Cu(I)'s cannot stay close to each other even if two Al's are located at the ideal distance, probably because of the strong electrostatic repulsion (Figure 4b). Our result therefore makes one doubt

the existence of a Cu dimer, although isolated Cu(I) may exist as is evidenced by many experiments. It should be noted that in the course of the simulation, Cu(I) moved back and forth from one adsorption structure to the other symmetrically equivalent one. This high mobility of Cu(I) may hinder the detection by EXAFS and may also allow the Cu(I)'s to approach each other momentarily. The vicinity of two Cu(I)'s was taken as a cluster model and was calculated by ab initio MO method in the singlet state. The overall structure of Cu(I) coordination obtained by the MO calculation (Figure 2c) was similar to that obtained by MD (Figure 4b), which proved the reliability of the MD simulation. Small discrepancies were, however, observed in the Cu–O bond length. MO predicted Cu–O distances 0.3–0.7 Å shorter than did MD. Further tuning of the Cu(I) parameter may yield a better agreement with the MO structure.

To calculate the photoluminescence spectra, the Cu(I) monomer and dimer were reoptimized in the triplet state. One thing to be pointed out with regard to the structure is that when optimized in triplet state, two Cu(I)'s form a dimer at the atomic distance of approximately 3 Å (Figure 5a). The reason for the dimerization was considered as follows. When Cu's electron is excited to a higher level, a hole is created, into which the electron of the surrounding zeolite oxygen flows. This is evidenced by the negative (Mulliken) atomic charge on Cu (−0.14 au). Thus the electrostatic repulsion between Cu's are reduced, or even an attractive interaction may work between Cu's which led to the formation of the dimer. Furthermore, if electron correlation is included in the calculations, which means to take into account the electronic configurations of the excited states in the sense of CI, the Cu(I) dimer may be found even in the ground state. In any cases, the potential well of Cu(I) dimer would be shallow and would not be stable at the elevated temperature. Calculated photoemission bands are 768 and 1392 nm for Cu(I) monomer and dimer, respectively, as compared to the experimentally detected peaks at 480 and 540 nm.⁸ Both calculated spectra underestimate the bandgap, which may be due to the inadequacy of the computation level, and hence a quantitative discussion cannot be made. However, even if one admits the inaccuracy of this calculation, the estimated wavelength of Cu dimer emission is too long to be assigned to the observed bands. Furthermore, Dedecek et al.⁸ assigned the 480 and 540 nm bands to Cu associated with Al pairs and single Al, respectively. Our calculation, on the contrary, predicted that Cu(I)'s near two Al sites will dimerize spontaneously upon the excitation, and the emission peak from this dimer will be much longer than that from Cu(I) associated with single Al. This result therefore defies the assignment of the observed two peaks to Cu(I) dimer and monomer. We infer that the observed two bands both corresponds to Cu(I) associated with single Al, but coordinated differently, e.g., coordination to the 5-membered ring vs 6-membered ring. Whatever, further characterization of Cu(I) dimer using the models as large as the present one and at higher computational level including electron correlation effect with the large basis set is waited for.

Finally, from the expectation that NO adsorption might promote the formation of Cu(I) dimer, the Cu(I) dimer bridged by NO through N and through O were studied. As mentioned in the result section, geometry optimization of both structures lead to the NO adsorbed on the single Cu(I) through O (Figure 6a). NO adsorption on the single Cu(I) through N was also examined for the comparison and found less stable than the adsorption through O by 3.1 kcal/mol. In both optimized structures, the positions of two Cu(I)'s were almost the same as those of two Cu(I)'s without NO. Therefore the influence

of NO adsorption on the Cu(I) coordination structure was suggested to be small. The preference of the adsorption through O contradicts to the previous calculations¹³ and is probably the artifact of the poor computation level underestimating the adsorption energy through N. Weaker interaction is also evidenced by the longer N—Cu bond length (2.14 Å) compared to the former report (1.74 Å).¹³ Therefore, again a higher level of calculation may be able to locate a Cu(I) dimer bridged by NO which, however, would not be stable at the working temperature. Thus the reaction mechanisms based on the Cu(I) dimer such as the ones proposed by Beutel⁷ and Iwamoto²² are strongly doubted.

Conclusion

The coordination of Cu ionic species in ZSM-5 zeolite was investigated by molecular dynamics simulations. When two Al's occupy T8 sites in the six-membered ring, the calculated structure reproduced the square-planar coordination of Cu(II). For this Al siting, Cu(II)—O—Cu(II) and Cu(I) were simulated, and the coordination of the former species was found to be consistent with the EXAFS data. Ab initio MO calculations were also performed using the cluster models based on the structures obtained by MD. Overall shapes were well preserved and the MD parameters used here were verified. The Cu—O—Cu species was found to possess a unique electronic structure and was expected to be highly reactive. The role of the zeolite may thus be to disperse these reactive species. The existence of the Cu(I) dimer was strongly questioned by MD simulation and photoluminescence calculation. Cu(I)'s did not approach each other even after NO is adsorbed. The reaction mechanism based on the Cu dimer is thus doubtful.

Acknowledgment. This work was carried out as an activity of the catalyst workshop organized by The Association for the Progress of New Chemistry (ASPRONC) in Japan. We thank Prof. M. Iwamoto of Hokkaido University for instructive discussions.

References and Notes

- (1) Iwamoto, M.; Furukawa, H.; Mine, Y.; Uemura, F.; Mikuriya, S.; Kagawa, S. *J. Chem. Soc., Chem. Commun.* **1986**, 1272.
- (2) Iwamoto, M.; Mizuno, N. *Shokubai* **1990**, 32, 462.
- (3) Kucherov, A. V.; Slinkin, A. A.; Kondratev, D. A.; Bondarenko, T. N.; Rubinstein, A. M.; Minachev, Kh. M. *Zeolites* **1985**, 5, 320.
- (4) Grünert, W.; Hayes, N. W.; Joyner, R. W.; Shpiro, E. S.; Siddiqui, M. R. H.; Beave, G. N. *J. Phys. Chem.* **1994**, 98, 10832.
- (5) Larsen, S. C.; Aylor, A.; Bell, A. T.; Reimer, J. A. *J. Phys. Chem.* **1994**, 98, 11533.
- (6) Dedecek, J.; Sobalik, Z.; Tvaruzkove, Z.; Kaucky, D.; Wichterlove, B. *J. Phys. Chem.* **1995**, 99, 16327.
- (7) Beutel, T.; Sarkany, J.; Lei, G.-D.; Yan, J. T.; Sachtler, M. H. *J. Phys. Chem.* **1996**, 100, 845.
- (8) Dedecek, J.; Wichterlowa, B. *J. Phys. Chem.* **1994**, 98, 5721.
- (9) Iwamoto, M.; Yahiro, H.; Misuno, N.; Zhang, W.-X.; Mine, Y.; Furukawa, H.; Kagawa, S. *J. Phys. Chem.* **1992**, 96, 9360.
- (10) Valyon, J.; Hall, W. K. *J. Phys. Chem.* **1993**, 97, 1204.
- (11) Sarkany, J.; Sachtler, W. M. H. *Zeolites* **1994**, 14, 7.
- (12) Sayle, D. C.; Perrin, M. A.; Nortier, P.; Catlow, C. R. A. *J. Chem. Soc., Chem. Commun.* **1995**, 945.
- (13) Yokomichi, Y.; Yamabe, T.; Ohtsuka, H.; Kakumoto, T. *J. Phys. Chem.* **1996**, 100, 14424.
- (14) Trout, B. T.; Chakraborty, A. K.; Bell, A. T. *J. Phys. Chem.* **1996**, 100, 17582.
- (15) Kawamura, K. *JCPE* P029
- (16) Gaussian 94, Revision B.2; M. J. Frisch, G. W. Trucks, H. B. Schlegel, P. M. W. Gill, B. G. Johnson, M. A. Robb, J. R. Cheeseman, T. Keith, G. A. Petersson, J. A. Montgomery, K. Raghavachari, M. A. Al-Laham, V. G. Zakrzewski, J. V. Ortiz, J. B. Foresman, J. Cioslowski, B. B. Stefanov, A. Nanayakkara, M. Challacombe, C. Y. Peng, P. Y. Ayala, W. Chen, M. W. Wong, J. L. Andres, E. S. Replogle, R. Gomperts, R. L. Martin, D. J. Fox, J. S. Binkley, D. J. Defrees, J. Baker, J. P. Stewart, M. Head-Gordon, C. Gonzalez, and J. A. Pople; Gaussian, Inc.: Pittsburgh, PA, 1995.
- (17) Derouane, E. G.; Fripiat, J. G. *Zeolites* **1985**, 5, 165.
- (18) Swaisgood, A. A.; Barr, M. K.; Hay, P. J.; Redondo, A. *J. Phys. Chem.* **1991**, 95, 10031.
- (19) Chatterjee, A.; Vetrivel, R. *Zeolites* **1994**, 14, 225.
- (20) Blanco, F.; Villalba, G. U.; Agudelo, M. M. R. *Mol. Simul.* **1995**, 14, 165.
- (21) Schröder, K. P.; Sauer, J.; Leslie, M.; Catlow, C. R. A. *Zeolites* **1992**, 12, 20.
- (22) Private communication with M. Iwamoto.